

Unusual Magnetic Property Associated with Dimerization within a Nickel Tetramer

Xiaoming Ren,[†] Qingjin Meng,^{*,†} You Song,[†] Chuanjiang Hu,[†] Changsheng Lu,[†] Xiaoyuan Chen,[‡] and Ziling Xue[§]

Coordination Chemistry Institute, State Key Laboratory of Coordination Chemistry, Nanjing University, Nanjing, 210093, P. R. China, Department of Chemistry, Syracuse University, Syracuse, New York 13244, and Department of Chemistry, Tennessee University, Knoxville, Tennessee 37996

Received March 12, 2002

A new ion-pair complex, 1-benzyl-4-aminopyridinium bis(maleonitriledithiolato)nickelate(III) (**1**), has been synthesized. The variable magnetic susceptibility results of **1** show a discontinuity around 184 K, which is phenomenologically similar to that observed for first-row transition metal complexes undergoing a spin crossover transition. The crystal structure analyses of **1** at high and low temperatures indicate that this unusual magnetic property is associated with a packing structure that changes from tetrameric spin clusters to dimers between neighboring spin carriers.

One-dimensional (1-D) molecular solids have attracted widespread attention because they show novel physical properties such as Peierls transition, spin-Peierls transition, charge density wave (CDW) states, spin density wave (SDW) states, molecular magnetic bistability, molecular magnetic nanowire, etc.¹ In addition, 1-D compounds have also stimulated theoretical investigations.

Among the most studied 1-D transition metal complexes are complexes containing $[M(\text{mnt})_2]^-$ ($M = \text{Ni(III)}, \text{Pd(III)}, \text{or Pt(III)}$) ions. In these compounds, the constituent planar molecules $[M(\text{mnt})_2]^-$ form columnar stacking, in which intermolecular d_{π}^2 or π orbital interactions result in a 1-D electronic nature.^{2–5} Generally, the topology and size of the

counteranion in $[M(\text{mnt})_2]^-$ complexes play an important role in controlling the stacks of anions and cations. We have recently developed a new class of salts $[\text{RbzPy}]^+[\text{Ni}(\text{mnt})_2]^-$ ($[\text{RbzPy}]^+ = \text{derivative of benzylpyridinium}$). Some significant and interesting results are described as follows:⁶ (1) The structural feature of this class of complexes is that the well-separated anions and cations form regular stacked columns in which $[\text{Ni}(\text{mnt})_2]^-$ anions form a 1-D magnetic chain of $S = 1/2$. (2) The topology and size of the $[\text{RbzPy}]^+$ ion, which is related to the molecular conformation of the $[\text{RbzPy}]^+$ ion, can be modified by systematic variation of the substituent groups in aromatic rings. Therefore, the stacking structure of those complexes can be finely tuned by controlling the molecular conformation of the $[\text{RbzPy}]^+$ ion. (3) These classes of 1-D chain complexes are strongly correlated electron systems, and magnetic interactions in these systems are very sensitive to intermolecular separations.

In this contribution, an ion-pair complex (**1**) with an unusual magnetic property, which consists of $[\text{Ni}(\text{mnt})_2]^-$ and 1-benzyl-4-aminopyridinium (Scheme 1), is described. Upon decreasing the temperature, the packing structure of **1** in the solid state converts from tetrameric spin clusters to the dimers. As a consequence, the temperature dependence of the magnetic susceptibility exhibits a discontinuity phenomenologically similar to that observed for first-row transition metal complexes undergoing a spin crossover transition. The transition feature has been characterized by magnetic susceptibility measurement, crystal structure de-

* Corresponding author. E-mail: Xmren@netra.nju.edu.cn.

[†] Nanjing University.[‡] Syracuse University.[§] Tennessee University.

- (1) (a) Coomber, A. T.; Beljonne, D.; Friend, R. H.; Brédas, J. L.; Charlton, A.; Robertson, N.; Underhill, A. E.; Kurmoo, M.; Day, P. *Nature* **1996**, *380*, 144. (b) Manabe, T.; Kawashima, T.; Ishii, T.; Matsuzaka, H.; Yamashita, M.; Mitani, T.; Okamoto, H. *Synth. Met.* **2001**, *116*, 415. (c) Wei, J. H.; Zhao, J. Q.; Liu, D. S.; Xie, S. J.; Mei, L. M.; Hong, J. *Synth. Met.* **2001**, *122*, 305. (d) Caneschi, A.; Gatteschi, D.; Lalioti, N.; Sangregorio, C.; Sessoli, R.; Venturi, G.; Vigningni, A.; Rettori, A.; Pini, M. G.; Novak, M. A. *Angew. Chem., Int. Ed.* **2001**, *40*, 1760. (e) Fujita, W.; Awaga, K. *Science* **1999**, *286*, 261. (f) Sugano, T. *Polyhedron* **2001**, *20*, 1285 and references therein. (g) Kommandeur, J.; Vegter, J. G. *Mol. Cryst. Liq. Cryst.* **1975**, *30*, 11. (h) Kosaki, A.; Sorai, M.; Suga, H.; Seki, S. *Bull. Chem. Soc. Jpn* **1977**, *50*, 810. (i) Hobi, M.; Zürcher, S.; Gramlich, V.; Burckhardt, U.; Mensing, C.; Spahr, M.; Togni, A. *Organometallics* **1996**, *15*, 5342.

- (2) Nishijo, J.; Ogura, E.; Yamaura, J.; Miyazaki, A.; Enoki, T.; Takano, T.; Kuwatani, Y.; Iyoda, M. *Solid State Commun.* **2000**, *116*, 661. (3) Pullen, A. E.; Faulmann, C.; Pokhodnya, K. I.; Cassoux, P.; Tokumoto, M. *Inorg. Chem.* **1998**, *37*, 6714. (4) Allan, M. L.; Coomber, A. T.; Marsden, I. R.; Martens, J. H. F.; Friend, R. H.; Charlton, A.; Underhill, A. E. *Synth. Met.* **1993**, *55–57*, 3317. (5) Kobayashi, A.; Sasaki, Y.; Kobayashi, H.; Underhill, A. E.; Ahmad, M. M. *J. Chem. Soc., Dalton Trans.* **1982**, 390. (6) (a) Ren, X. M.; Lu, C. S.; Liu, Y. J.; Zhu, H. Z.; Li, H. F.; Hu, C. J.; Meng, Q. J. *Transition Met. Chem.* **2001**, *26* (1/2), 136. (b) Ren, X. M.; Li, H. F.; Wu, P. H.; Meng, Q. J. *Acta Crystallogr., Sect. C* **2001**, *C57*, 1022. (c) Ren, X. M.; Meng, Q. J.; et al. Submitted to *Inorg. Chem.* (d) Unpublished materials.

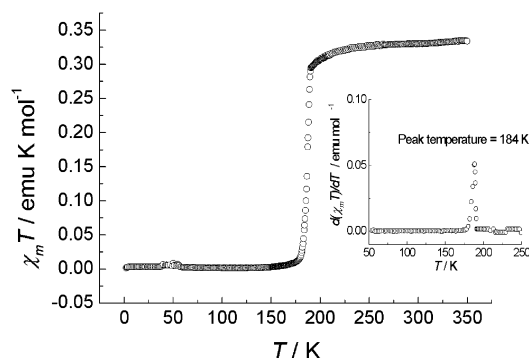
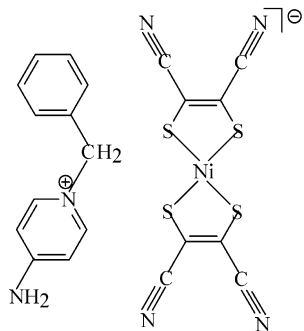


Figure 1. The plot of $\chi_m T$ versus T for **1**. Inset: $d(\chi_m T)/dT$ versus T .

Scheme 1. Molecule Structure of **1**



termination in high- and low-temperature phases, and DSC analysis.

The starting materials, Na_2mnt and [1-benzyl-4-aminopyridinium]Cl, were synthesized by the literature procedures.^{7,8} A similar method for preparing $[\text{Bu}_4\text{N}]_2[\text{Ni}(\text{mnt})_2]$ was utilized to prepare $[\text{1-benzyl-4-aminopyridinium}]_2[\text{Ni}(\text{mnt})_2]$. **1** was prepared by the reaction of 1.0 equiv of [1-benzyl-4-aminopyridinium]₂[Ni(mnt)₂] with 0.6 equiv of I_2 in MeCN–MeOH mixed solution. Single crystals suitable for the X-ray structure analysis were obtained by diffusing Et_2O into **1** solution in MeCN.

Magnetic susceptibilities were measured with a Quantum Design MPMS-5S superconducting quantum interference device (SQUID) magnetometer in the range 2–350 K. The diamagnetic correction was evaluated by using Pascal's constants.

A plot of $\chi_m T$ versus T for **1** is shown in Figure 1. The $\chi_m T$ value per mole of **1** at 350 K is $0.340 \text{ emu} \cdot \text{K} \cdot \text{mol}^{-1}$, and slightly lower than that expected for independent $S = 1/2$. As a sample **1** was cooled from 350 K, the $\chi_m T$ value first decreases smoothly, then abruptly at 188 K, before dropping to zero around 145 K. Below this temperature, this complex is diamagnetic. When the temperature is increased from 2 to 350 K, an identical curve is observed with no hysteresis effect. Around 184 K, which is the temperature at the sharp peak of $d(\chi_m T)/dT$ shown in the inset of Figure 1, the value of $\chi_m T$ abruptly drops from 0.295 to $0.018 \text{ emu} \cdot \text{K} \cdot \text{mol}^{-1}$ within 10 K. The material thus exhibits a switching from paramagnetic to diamagnetic around 184 K.

(7) Davison, A.; Holm, H. R. *Inorg. Synth.* **1967**, *10*, 8.

(8) Bulgarevich, S. B.; Bren, D. V.; Movshovic, D. Y.; Finocchiaro, P.; Failla, S. *J. Mol. Struct.* **1994**, *317*, 147.

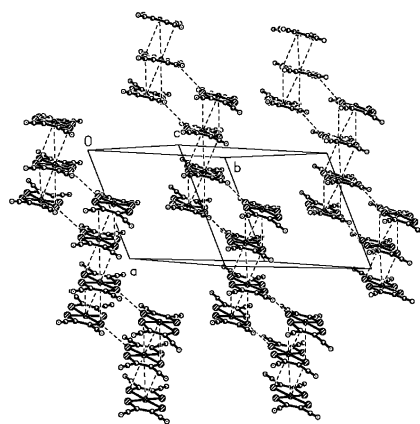


Figure 2. The subunit of BAAB consisted of $[\text{Ni}(\text{mnt})_2]^-$ anions and the infinite chains formed by $\text{S} \cdots \text{S}$ interactions.

A crystal structure analysis⁹ of **1** at 293 K [high-temperature phase (HT phase)] shows that an asymmetric unit in a cell comprises two $[\text{Ni}(\text{mnt})_2]^-$ anions and two [1-benzyl-4-aminopyridinium]⁺ cations. Most of the bond lengths and bond angles are in agreement with those in other $[\text{Ni}(\text{mnt})_2]^-$ complexes,⁶ except that the N atoms of the CN group in $[\text{Ni}(\text{mnt})_2]^-$ anions have unusual deviations from S_4 planes. The average deviation containing Ni(1) anion is around 0.1 Å, and the deviation containing Ni(2) anion is around 0.32 Å. The anions are stacked face-to-face along the a -axis (Figure 2) to form a 4-fold anion subunit. In each subunit, the stacking is regular, and the overlap of the neighboring anion is slightly shifted. The two independent Ni \cdots Ni distances in the 4-fold subunit are 3.946 and 3.950 Å, respectively. The conformations of two [1-benzyl-4-aminopyridinium]⁺ cations are slightly different, and the pyridine ring and benzene ring with the $\text{C}_{\text{Bz}}-\text{C}-\text{N}_{\text{Py}}$ reference plane in two [1-benzyl-4-aminopyridinium]⁺ cations make dihedral angles of 105.5°, 89.8° and 96.5°, 84.3°, respectively.

The molecular structure of **1** at 89 K [the low-temperature phase (LT phase)] is similar to that at 293 K, except that the molecular packing in the LT phase is significantly different from that in the HT phase (Figure 3).

The nearest-neighbor intermolecular arrangements [Ni(1) anion \cdots Ni(2A) anion, and Ni(1A) anion \cdots Ni(2B) anion] exhibit a farther slipped overlap in the HT phase compared

(9) Crystal data ($\text{C}_{20}\text{H}_{13}\text{N}_6\text{NiS}_4$): $T = 293(2) \text{ K}$, triclinic, space group $P1$, $a = 11.220(2) \text{ Å}$, $b = 14.295(3) \text{ Å}$, $c = 15.609(3) \text{ Å}$, $\alpha = 74.00(3)^\circ$, $\beta = 77.30(3)^\circ$, $\gamma = 68.04(3)^\circ$, $V = 2212.7(8) \text{ Å}^3$, $Z = 4$, $\rho_{\text{calcd}} = 1.574 \text{ g} \cdot \text{cm}^{-3}$; FR590 CAD4 diffractometer, Mo $K\alpha$ radiation $\lambda = 0.71073 \text{ Å}$; 8027 measured ($1.37^\circ \leq \theta \leq 24.97^\circ$) and 7766 independent reflections used in the refinement; Lorentz polarization but no absorption corrections ($\mu = 1.275 \text{ mm}^{-1}$). The structure was solved by direct methods by using SHELXS 97 and refined with SHELXL 97, 559 parameters. $R1(\text{on } F^2) = 0.0322$, $wR2(\text{on } F^2) = 0.0996$, residual electron density $0.324 \text{ e} \cdot \text{Å}^{-3}$. $T = 89(3) \text{ K}$, triclinic, space group $P1$, $a = 11.3376(15) \text{ Å}$, $b = 13.9757(18) \text{ Å}$, $c = 15.481(2) \text{ Å}$, $\alpha = 73.070(2)^\circ$, $\beta = 74.367(2)^\circ$, $\gamma = 67.640(2)^\circ$, $V = 2135.1(5) \text{ Å}^3$, $Z = 4$, $\rho_{\text{calcd}} = 1.631 \text{ g} \cdot \text{cm}^{-3}$; CCD area detector, Mo $K\alpha$ radiation $\lambda = 0.71073 \text{ Å}$; 9653 measured ($1.9^\circ \leq \theta \leq 28.29^\circ$) and 7442 independent reflections used in the refinement; Lorentz polarization but no absorption corrections ($\mu = 1.321 \text{ mm}^{-1}$). The structure was solved by direct methods by using SHELXS 97 and refined with SHELXL 97, 575 parameters. $R1(\text{on } F^2) = 0.0316$, $wR2(\text{on } F^2) = 0.0809$, residual electron density $0.545 \text{ e} \cdot \text{Å}^{-3}$.

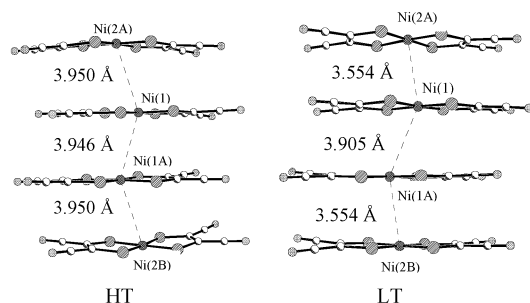


Figure 3. The side views of the 4-fold anion subunit in the HT and LT phases. Symmetric codes: 1A = $2 - x, 1 - y, 1 - z$; 2A = $1 - x, 1 - y, 1 - z$; 2B = $1 + x, y, z$.

with that in the LT phase.^{1e} The distance of Ni(1)···Ni(2A) and Ni(1A)···Ni(2B) in the LT phase is reduced by 0.4 Å (from 3.950 Å in the HT phase to 3.554 Å in the LT phase), and the distance of Ni(1)···Ni(1A) in the LT phase is reduced only by 0.04 Å. The geometry in the LT phase maximizes the exchange energy because of the better overlap between the unlocalized electrons on the $[\text{Ni}(\text{mnt})_2]^-$ anions.^{1e} As a consequence, there are stronger interactions between Ni(1) and Ni(2A), Ni(1A) and Ni(2B) to form a dimer structure in the LT phase. The conformations of two cations in the LT phase are slightly different from those in the HT phase; the pyridine ring and benzene ring with the $\text{C}_{\text{Bz}}-\text{C}-\text{N}_{\text{Py}}$ reference plane in two cations make dihedral angles of 104.5°, 88.7° and 96.3°, 80.7°, respectively. It is noted that the crystallographic phase transition from the HT phase to the LT phase is accompanied by a paramagnetic to diamagnetic switching.

Differential scanning calorimetry (DSC) measurements were performed with a Perkin-Elmer calorimeter in the temperature range 93–293 K (−180 to 20 °C). The power-compensated DSC trace at the warming rate 20 K min^{−1} is shown in Figure 4. At 191 K, which is near the phase transition temperature obtained from magnetic susceptibility measurements, an endothermic effect of this phase transition was observed, and the enthalpy change, ΔH , was 1.52 kJ·mol^{−1}. The result of DSC indicated that the enthalpy and entropy are discontinuous when this sample changes from one phase to another phase; the phase transition is thus first order.

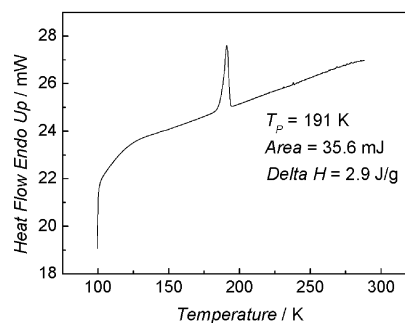


Figure 4. DSC of **1** showing the phase transition at 191 K (peak temperature).

In conclusion, a complex with a phenomenologically spin-transition-like nature has been characterized by magnetic susceptibility measurements, its crystal structure determination in both HT and LT phases, and DSC analyses. The abrupt change of the temperature dependence of the magnetic susceptibility is associated with packing structure changing from tetrameric spin clusters to dimers between neighboring spin carriers, and shows feature of spin switching. The DSC analyses further indicate that the phase transition is first order. These results in current study reveal a magnetic switching feature from paramagnetic to diamagnetic as the result of a crystallographic phase transition. Such systems may potentially be used in molecular devices.

Acknowledgment. The authors thank Prof. Q. P. Dai and Ms. Z. R. Yuan of DSC Lab in the center of analysis and determining of Nanjing University for determining DSC data and acknowledge funding from the National Natural Science Foundation and the State Education Commission of China.

Supporting Information Available: Characterization data and detailed descriptions of the synthesis of **1**, tables of crystal data, structure solution and refinement, atomic coordinates, bond lengths and angles, and anisotropic thermal parameters for **1** in the HT and LT phases (PDF). X-ray crystallographic files (CIF). This material is available free of charge via the Internet at <http://pubs.acs.org>.

IC0255860